

OPEN

Analysis of L-arginine:glycine amidinotransferase-, creatine- and homoarginine-dependent gene regulation in the murine heart

Märit Jensen^{1,3}, Christian Müller^{1,2}, Chi-un Choe^{2,3}, Edzard Schwedhelm^{2,4} & Tanja Zeller^{1,2*}

L-arginine:glycine amidinotransferase (AGAT) and its metabolites creatine and homoarginine (HA) have been linked to cardiovascular pathologies in both human and murine studies, but the underlying molecular mechanisms are poorly understood. Here, we report the first analysis of heart transcriptome variation using microarrays in an AGAT-deficient (AGAT^{-/-}) mouse model to evaluate AGAT-, creatine- and HA-dependent gene regulation. Our data revealed significant differences of gene expression between AGAT^{-/-} and wild-type (WT) mice, affecting cardiac energy metabolism (*Fbp2*, *Ucp2*), cardiac hypertrophy and fibrosis (*Nppa*, *Ctgf*), immune response (*Fgl2*), and the conduction system of the heart (*Dsc2*, *Ehd4*, *Hcn2*, *Hcn4*, *Scn4a*, *Scn4b*). All of these genes being expressed on WT level in creatine-supplemented mice. Using *in silico* analysis based on the GEO database we found that most of these candidate genes (*Ctgf*, *Dsc2*, *Fbp2*, *Fgl2*, *Hcn2*, *Nppa*) revealed significant alterations in a WT mouse model of myocardial infarction underlining a pathophysiological relationship between AGAT metabolism and cardiovascular disease.

Cardiovascular disease (CVD) is one of the major causes of death and hospitalization in the world¹. Current risk stratification is mainly based on classical risk factors such as hypertension, smoking, hypercholesterolemia, obesity and diabetes. However, these factors do not include the molecular and metabolic factors which reflect the complex and heterogenic etiology of CVD. Several epidemiological studies in the cardiovascular field identified novel biomarkers to predict clinical outcome and provide a better understanding of disease progression. In particular, metabolic pathways in CVD represent potential new valuable targets for drug therapy^{2,3}.

The L-arginine derivative L-homoarginine (HA) and the nitrogenous organic acid creatine are part of one such pathway and have been investigated with regard to CVD. HA was identified as a prognostic factor for CVD. Several studies revealed a correlation between low HA plasma levels and an increased cardiovascular mortality, e.g., after myocardial infarction (MI), in heart failure and after ischemic stroke⁴⁻⁶. Moreover, HA is involved in nitric oxide (NO) metabolism and inhibits alkaline phosphatase at high concentrations linking it to vascular function and atherosclerosis^{7,8}. Creatine on the other hand, plays a key role in cardiac energy metabolism and acts as a rapidly available energy buffer by its involvement in the recycling of adenosine triphosphate (ATP)⁹. It has been shown that all major components of this system including creatine are down-regulated in the failing heart^{10,11}.

The common enzyme for endogenous HA and creatine formation is the L-arginine:glycine amidinotransferase (AGAT; EC: 2.1.4.1). In humans, single-nucleotide polymorphisms (SNPs) within the *AGAT* gene are associated with variations of HA plasma concentrations^{12,13}. For the leading SNP rs1288775 (*AGAT* missense), homozygous allele carriers of the minor allele had significantly higher plasma HA compared with heterozygous or homozygous allele carriers of the major allele, representing a gene dose-dependent effect^{12,13}. Previously we have generated AGAT-deficient (AGAT^{-/-}) mice which showed whole body HA and creatine deficiency^{12,14}. These AGAT^{-/-} mice exhibited a cardiovascular phenotype of low left ventricular end-systolic pressure (LVESP),

¹University Heart and Vascular Centre Hamburg, Clinic for Cardiology, University Medical Centre Hamburg-Eppendorf, Hamburg, 20246, Germany. ²German Centre for Cardiovascular Research (DZHK e.V.), partner site Hamburg/Kiel/Lübeck, Hamburg, 20246, Germany. ³Department of Neurology, University Medical Centre Hamburg-Eppendorf, Hamburg, 20246, Germany. ⁴Institute of Clinical Pharmacology and Toxicology, University Medical Centre Hamburg-Eppendorf, Hamburg, 20246, Germany. *email: t.zeller@uke.de

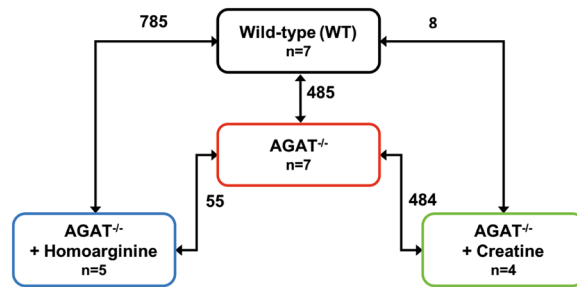


Figure 1. Number of differentially expressed genes between the groups in murine heart tissue. Transcriptome profiling was performed using the Affymetrix Mouse GeneChip 1.0 ST Array. Each line indicates the comparison of the respective two groups and the number of significantly regulated genes. Significance level: False-Discovery-Rate (FDR) ≤ 0.05 . Abbreviations: WT, wild-type; AGAT^{-/-}, AGAT knock-out; n, number of animals.

Gene	Gene name	P Value	FC
<i>Scn4a</i>	sodium channel, voltage-gated, type IV, alpha	3.02×10^{-13}	-3.22
<i>Scn4b</i>	sodium channel, type IV, beta	1.47×10^{-12}	-3.74
<i>Tmod4</i>	tropomodulin 4	8.93×10^{-11}	-1.76
<i>Tmem150c</i>	transmembrane protein 150 C	9.97×10^{-11}	-2.96
<i>Fah</i>	fumarylacetoacetate hydrolase	1.08×10^{-10}	-2.36
<i>Agat</i>	L-arginine:glycine amidinotransferase	1.18×10^{-10}	-2.19
<i>Lgi1</i>	leucine-rich repeat LGI family, member 1	2.07×10^{-10}	-3.10
<i>Lad1</i>	ladinin	2.63×10^{-10}	2.17
<i>Stom</i>	stomatin	1.12×10^{-9}	-1.41
<i>Zfp106</i>	zinc finger protein 106	1.31×10^{-9}	1.49
<i>Egf</i>	epidermal growth factor	6.62×10^{-9}	-1.55
<i>Ndr4</i>	N-myc downstream regulated gene 4	9.12×10^{-9}	1.44
<i>Vwa8</i>	von Willebrand factor A domain containing 8	1.20×10^{-8}	-1.35
<i>Ano5</i>	anoctamin 5	1.78×10^{-8}	-2.27
<i>Slc16a7</i>	solute carrier family 16 (monocarboxylic acid transporters), member 7	1.97×10^{-8}	1.70
<i>Ivd</i>	isovaleryl coenzyme A dehydrogenase	2.54×10^{-8}	-1.41
<i>Hn1</i>	hematological and neurological expressed sequence 1	2.60×10^{-8}	1.41
<i>Nr0b2</i>	nuclear receptor subfamily 0, group B, member 2	3.93×10^{-8}	1.47
<i>Slc22a3</i>	solute carrier family 22 (organic cation transporter), member 3	3.99×10^{-8}	-1.66
<i>Acsm5</i>	acyl-CoA synthetase medium-chain family member 5	4.32×10^{-8}	-1.88

Table 1. Top 20 differentially expressed genes between WT and AGAT^{-/-} mice in heart tissue. False-Discovery-Rate ≤ 0.05 . Abbreviations: FC, fold change.

impaired contractility and relaxation, as well as a lower maximal heart rate and contractile reserve in response to dobutamine infusion compared to wild-type (WT) mice¹⁵. Creatine supplementation corrected LVESP, while HA supplementation rescued all other hemodynamic parameters¹⁵. In a model of post-myocardial infarction, HA supplementation normalized several cardiac parameters in WT mice (i.e., relaxation, cardiac reserve)¹⁶. However, data on the underlying molecular mechanisms and signal transduction pathways in the AGAT metabolism are scant.

In this study we analysed the cardiac transcriptome of left ventricular tissue of WT mice, untreated AGAT^{-/-} mice and AGAT^{-/-} mice with creatine (AGAT^{-/-}-Cr) or HA (AGAT^{-/-}-HA) supplementation. The aim of our study was to identify molecular pathways and cardiovascular candidate genes related to AGAT and creatine or HA supplementation. Additionally, candidate genes were evaluated in a WT mouse model of MI using GEO data.

Results

Cardiac gene expression is altered in AGAT^{-/-} mice. We performed a transcriptome analysis of left ventricular tissue of WT, AGAT^{-/-}, AGAT^{-/-}-Cr and AGAT^{-/-}-HA mice in heart samples. The number of differentially expressed genes was evaluated for each comparison (Fig. 1).

Comparison of WT and AGAT^{-/-} mice revealed 485 significantly de-regulated genes (FDR ≤ 0.05 ; see Supplementary Table S1). The top 20 most up- and down-regulated genes are shown in Table 1. A heatmap of the top 50 de-regulated genes is displayed in Fig. 2. Differentially expressed genes were enriched for pathways (WikiPathways) involved in energy metabolism such as mitochondrial LC-fatty acid beta-oxidation

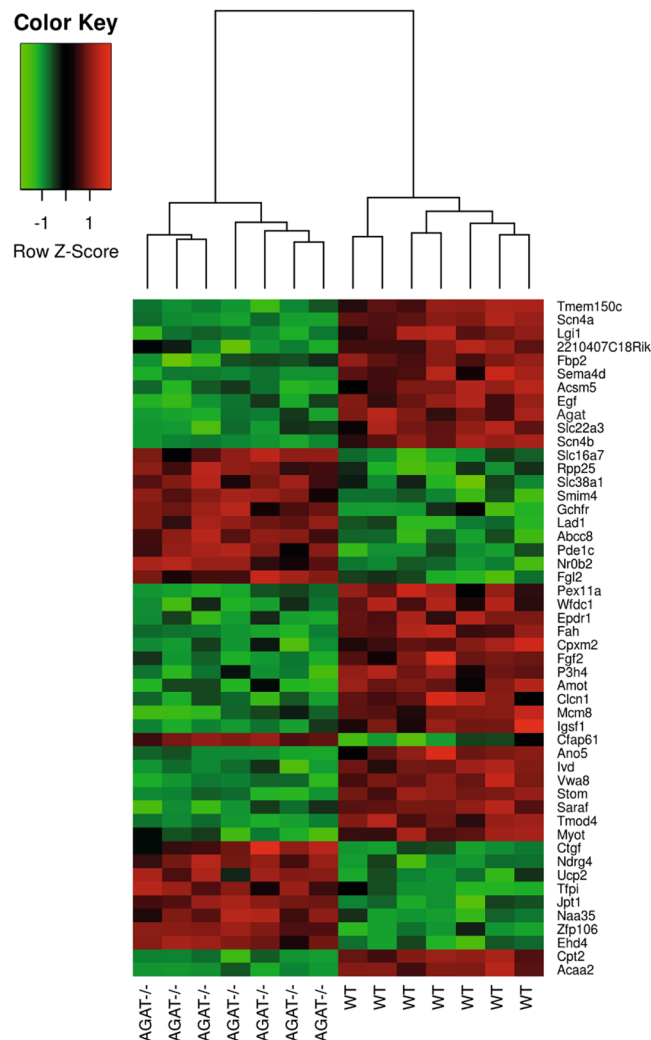


Figure 2. Heatmap of gene expression values depicting clustering of genes between WT and AGAT^{-/-} heart tissue samples. The heatmap is based on the expression of mRNAs for the set of the top 50 significant genes. Low to high expression is represented by a change of color from green to red, respectively. Abbreviations: AGAT^{-/-}, AGAT knock-out mice; WT, wild-type mice.

($P = 1.76 \times 10^{-9}$), fatty acid beta-oxidation ($P = 4.12 \times 10^{-9}$) and glycogen metabolism ($P = 8.03 \times 10^{-6}$). At the level of individual genes, the majority of genes involved in beta-oxidation were down-regulated in AGAT^{-/-} mice. An enrichment of genes involved in cardiac calcium regulation ($P = 4.32 \times 10^{-7}$) indicates a relation of these genes to cardiovascular metabolism (see Supplementary Fig. S1).

Creatine and HA have beneficial effects in AGAT^{-/-} mice on cardiac function¹⁵. Therefore, we analysed gene regulation in hearts of AGAT^{-/-} mice after either creatine or HA supplementation. We identified eight genes that were significantly different between WT and AGAT^{-/-}Cr littermates (i.e., 2% of AGAT-dependent de-regulated genes; $FDR \leq 0.05$). Thus, it can be assumed that the majority of de-regulated genes in the heart are creatine dependent. In AGAT^{-/-}HA mice, 785 ($FDR \leq 0.05$) genes were significantly de-regulated compared with expression levels in WT mice. 281 AGAT-dependent genes (i.e., 58%) remained differentially expressed in AGAT^{-/-}HA mice compared to WT mice. Considering that more genes were differentially expressed between WT and AGAT^{-/-}HA mice than between WT and AGAT^{-/-} littermates (785 vs. 485 genes, respectively), it can be assumed that HA supplementation and AGAT^{-/-} have an additive effect on changes seen for gene expression as compared with WT animals.

Network analysis reveals AGAT-dependent candidate genes. To detect important genes within the AGAT metabolism, we constructed modules of highly correlated genes by weighted correlation network analysis (WGCNA). Figure 3 shows the top two networks with the strongest association to the AGAT knock-out. The entire list of genes in Network 1 and 2 can be found as Supplementary Tables S2 and S3. Of these genes, candidates were selected based on 1.) known association with CVD and 2.) statistical significance (Table 2).

We first looked for genes with association to the cardiovascular system that have been discussed in literature. Among those genes are six well known CVD-associated genes. These include sodium voltage-gated channel alpha subunit 4 (*Scn4a*, $P = 3.02 \times 10^{-13}$), sodium voltage-gated channel beta subunit 4 (*Scn4b*, $P = 1.47 \times 10^{-12}$),

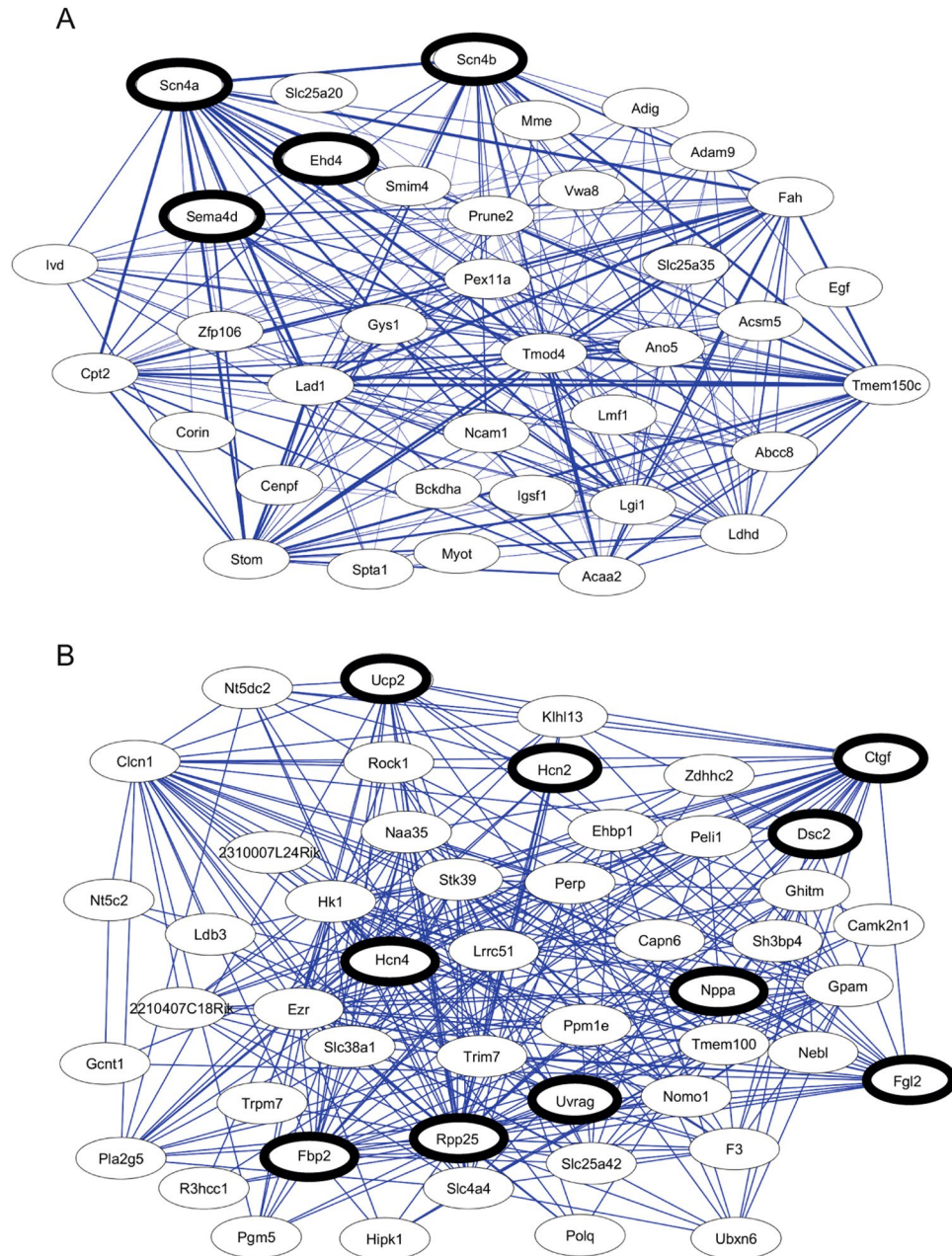


Figure 3. Network analysis between WT and AGAT^{-/-} mice in heart tissue. Differentially expressed genes were clustered into modules of highly co-expressed genes. The networks with the strongest associations are shown (A, $P = 1.07 \times 10^{-8}$; B, $P = 4.39 \times 10^{-8}$). Candidate genes (black circles) were selected based on 1.) known association with CVD and 2.) statistical significance.

and hyperpolarization-activated cyclic nucleotide-gated ion channel 4 (*Hcn4*, $P = 2.93 \times 10^{-4}$), which were all down-regulated in AGAT^{-/-} mice. Connective tissue growth factor (*Ctgf*, $P = 5.21 \times 10^{-7}$), natriuretic peptide type A (*Nppa*, $P = 1.17 \times 10^{-5}$) and hyperpolarization-activated cyclic nucleotide-gated ion channel 2 (*Hcn2*, $P = 1.48 \times 10^{-5}$) were found to be up-regulated in AGAT^{-/-} mice.

In addition, the results revealed that uncoupling protein 2 (*Ucp2*, $P = 3.49 \times 10^{-7}$), EH domain-containing protein 4 (*Ehd4*, $P = 6.03 \times 10^{-8}$), Semaphorin-4D (*Sema4d*, $P = 8.91 \times 10^{-8}$), fibrinogen like 2 (*Fgl2*, $P = 3.1 \times 10^{-7}$), Desmocollin 2 (*Dsc2*, $P = 4.33 \times 10^{-5}$) and UV radiation resistance associated gene (*Uvrag*, $P = 3.45 \times 10^{-4}$) were already linked to cardiovascular pathologies (see Table 2).

The top two significant genes within network 1 and 2 were *Scn4a* and *Scn4b* as well as ribonuclease P protein subunit p25 (*Rpp25*, $P = 8.71 \times 10^{-8}$) and fructose-1,6-bisphosphatase isozyme 2 (*Fbp2*, $P = 1.06 \times 10^{-7}$).

The majority of our candidate genes have been validated by qPCR. No significant de-regulation was found for *Sema4d* and *Uvrag* (Fig. 4). Thus, we excluded these genes from further analysis. As expected from microarray analysis, comparison of WT and AGAT^{-/-}Cr mice revealed that creatine supplementation leads to a restoration

Gene	WT vs. AGAT ^{-/-}		WT vs. AGAT ^{-/-} Cr		WT vs. AGAT ^{-/-} HA		References
	P Value	FC	P Value	FC	P Value	FC	
<i>Ctgf</i> ⁺	5.21 × 10 ⁻⁷	1.78	3.1 × 10 ⁻³	-1.33	1.36 × 10 ⁻⁷	1.83	Ohnishi <i>et al.</i> ²³ , Ahmed <i>et al.</i> ²⁴ , Oemar <i>et al.</i> ²⁵ , Koshman <i>et al.</i> ²⁶
<i>Dsc2</i> ⁺	4.33 × 10 ⁻⁵	1.35	NS	-1.07	NS	1.10	Sun <i>et al.</i> ²⁵ , Brodehl <i>et al.</i> ³⁶
<i>Ehd4</i> ⁺	6.03 × 10 ⁻⁸	1.36	NS	-1.04	3.15 × 10 ⁻⁶	1.34	Dun <i>et al.</i> ³⁴
<i>Fbp2</i> ⁺	1.06 × 10 ⁻⁷	-1.57	1.64 × 10 ⁻²	-1.12	4.66 × 10 ⁻⁷	-1.46	—
<i>Fgl2</i> ⁺	3.1 × 10 ⁻⁷	1.44	2.69 × 10 ⁻³	-1.2	3.65 × 10 ⁻²	1.15	Zhenzhong <i>et al.</i> ³⁷
<i>Hcn2</i> ⁺	1.48 × 10 ⁻⁵	1.33	9.67 × 10 ⁻³	-1.17	2.57 × 10 ⁻³	1.2	Robinson <i>et al.</i> ³⁰ , Vaccari <i>et al.</i> ³²
<i>Hcn4</i> ⁺	2.93 × 10 ⁻⁴	-1.42	NS	-1.07	8.8 × 10 ⁻³	-1.28	Robinson <i>et al.</i> ³⁰ , DiFrancesco <i>et al.</i> ³¹ , Baruscotti <i>et al.</i> ³³
<i>Nppa</i> ⁺	1.17 × 10 ⁻⁵	1.93	NS	1.02	1.16 × 10 ⁻²	1.55	Wang <i>et al.</i> ²²
<i>Rpp25</i> ⁺	8.71 × 10 ⁻⁸	1.69	NS	1	2 × 10 ⁻⁵	1.57	—
<i>Scn4a</i> ^{+,#}	3.02 × 10 ⁻¹³	-3.22	NS	-1.13	6.63 × 10 ⁻¹¹	-2.81	Coronel <i>et al.</i> ²⁷ , Lau <i>et al.</i> ²⁸
<i>Scn4b</i> ^{+,#}	1.47 × 10 ⁻¹²	-3.74	NS	1.12	6.13 × 10 ⁻⁸	-3.34	Li <i>et al.</i> ²⁹
<i>Sema4d</i> ⁺	8.91 × 10 ⁻⁸	-1.36	2.76 × 10 ⁻²	-1.13	2.4 × 10 ⁻⁷	-1.43	Willner <i>et al.</i> ⁴⁴
<i>Ucp2</i> ⁺	3.49 × 10 ⁻⁷	1.85	NS	-1.13	8.67 × 10 ⁻⁶	1.53	Saleh <i>et al.</i> ²⁰ , Akhmedov <i>et al.</i> ²¹
<i>Uvrag</i> ⁺	3.45 × 10 ⁻⁴	1.14	NS	-1.03	NS	1.05	Song <i>et al.</i> ⁴⁵

Table 2. AGAT-related candidate genes. Genes were selected based on 1. known association with CVD⁺ and 2. statistical significance[#]. For genes selected based on known association with CVD the according reference is given. False-Discovery-Rate ≤ 0.05. Abbreviations: FC, fold change; NS, not significant.

of gene expression levels towards WT levels. Comparing the expression levels of candidates between WT and AGAT^{-/-}HA mice, we found that most candidate genes remained differentially expressed.

Candidate genes are de-regulated in a mouse model of myocardial infarction. Since AGAT and HA/creatinine metabolism has been linked to MI and heart failure in both human and mice^{4-6,16}, we performed *in silico* gene expression analysis in a mouse model of MI to test our candidate genes in response to MI. For this, we used the publicly available GEO dataset GSE775¹⁷. WT mice were subjected either to MI by ligation of the left coronary artery or the sham operation, and gene expression between both groups was compared at six time points after MI. Among the 12 validated candidate genes, expression data were available for *Ctgf*, *Dsc2*, *Fbp2*, *Fgl2*, *Hcn2*, *Nppa* and *Ucp2* (Fig. 5). *Ctgf*, *Fgl2* and *Nppa* mRNA expression was significantly up-regulated at various time points post-MI, while gene expression of *Dsc2*, *Fbp2* and *Hcn2* was down-regulated in MI mice compared with sham-operated mice. Expression levels of *Ucp2* were not altered in the infarcted heart.

Discussion

The identification of unknown molecular mechanisms in CVD is needed to develop novel therapeutic strategies. In this context, the enzyme AGAT is of great importance since it is responsible for endogenous creatine and HA formation⁵. A lack of creatine results in altered cardiac energy metabolism^{10,11} and low HA plasma levels are associated with poor prognosis in CVD¹⁸. In this work we present transcriptomic variations linking AGAT, creatine and HA with its implications in cardiac (dys)function and CVD. As a main result we found that AGAT^{-/-} mice exhibited altered gene expression related to energy metabolism (*Fbp2*, *Ucp2*), cardiac hypertrophy and fibrosis (*Nppa*, *Ctgf*), immune response (*Fgl2*), and the conduction system of the heart (*Dsc2*, *Ehd4*, *Hcn2*, *Hcn4*, *Scn4a*, *Scn4b*). Notably, all of these genes being expressed on WT level in creatine-supplemented mice.

Our data revealed a widespread effect of the AGAT^{-/-} genotype on cardiac gene expression. This data complements with our previous cardiac phenotype studies that showed an impaired cardiac function in AGAT^{-/-} mice¹⁵. Pathway analysis of genes differentially expressed between WT and AGAT^{-/-} animals revealed that genes were enriched in energy metabolism pathways, such as mitochondrial LC-fatty acid beta-oxidation, fatty acid beta-oxidation and glycogen metabolism. This link between AGAT deficiency and energy metabolism, evidenced by diminished intracellular energy stores i.e., ATP and phosphocreatine (PCr) in brain and skeletal muscle, had been described previously^{9,14}. However, while PCr was completely absent in AGAT^{-/-} hearts, ATP remained at WT level¹⁵. Thus, AGAT^{-/-} mice seem to be able to maintain cardiac ATP production and storage through ATP synthesis pathways independent of the creatine/PCr system. Our analysis did not uncover alternative mechanisms of ATP synthesis as the majority of genes involved in beta-oxidation were down-regulated in AGAT^{-/-} mice. Therefore, further research is required to assess which mechanisms of ATP synthesis are responsible.

In addition, pathway analysis suggested an explanation for the observed association of AGAT deficiency and cardiac contractility, as cardiac calcium regulation was represented within the top ten pathways. Calcium is a critical regulator of cardiac myocyte function and the essential link in excitation contraction coupling¹⁹. De-regulation of cytoplasmic calcium leads to cardiac dysfunction, i.e., impaired contractility and relaxation and reduced inotropic reserve. This finding needs to be further experimentally addressed. Nevertheless, we provided a first hint to molecular mechanisms that could explain altered cardiac function in our AGAT^{-/-} mice as shown previously¹⁵.

Inspecting all genes included in the network analysis of differentially expressed genes between WT and AGAT^{-/-} mice, we found 14 candidate genes for changes in cardiovascular function of AGAT^{-/-} animals (*Ctgf*,

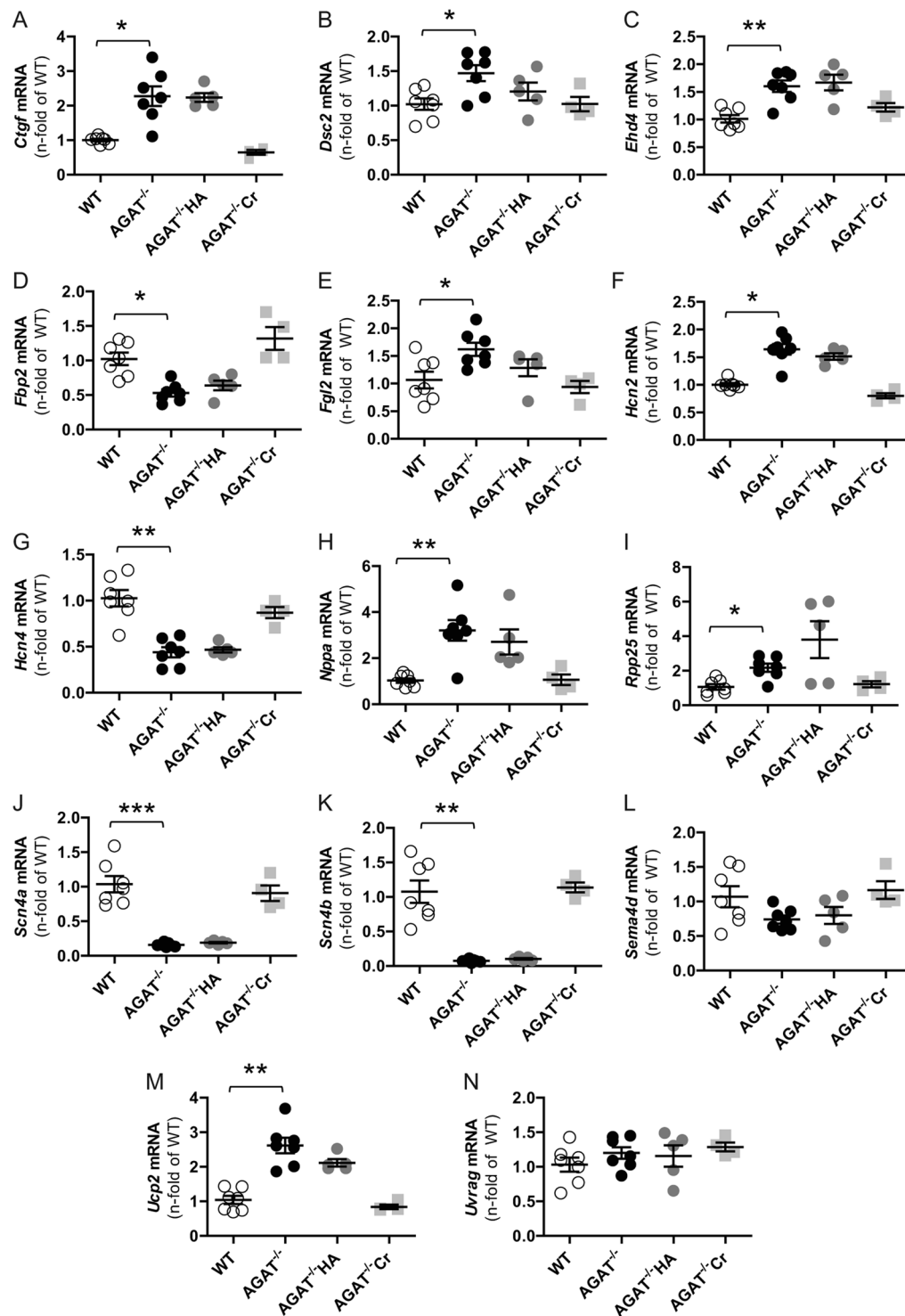


Figure 4. Validation of candidate genes by qPCR. Relative mRNA expression of candidate genes in the heart identified based on known association to the cardiovascular system and statistical significance. Each data point represents an individual mouse. Values are expressed as mean ± SEM. *P < 0.05, **P < 0.01 and ***P < 0.001 versus WT, Kruskal-Wallis-Test. WT (n = 7), AGAT^{-/-} (n = 7), AGAT^{-/-}HA (n = 5), AGAT^{-/-}Cr (n = 4).

Dsc2, *Ehd4*, *Fbp2*, *Fgl2*, *Hcn2*, *Hcn4*, *Nppa*, *Rpp25*, *Scn4a*, *Scn4b*, *Sema4d*, *Ucp2* and *Uvrag*). We excluded *Sema4d* and *Uvrag* from further analysis as validation by qPCR showed no significant AGAT-dependent regulation of these genes.

AGAT itself is an important regulator of energy homeostasis. Other individual energy related genes that might be additionally affected by AGAT deficiency comprise *Fbp2*, encoding for a gluconeogenesis enzyme, and *Ucp2*, encoding for a member of the family of inner mitochondrial membrane proteins. UCP2 is involved in lipid

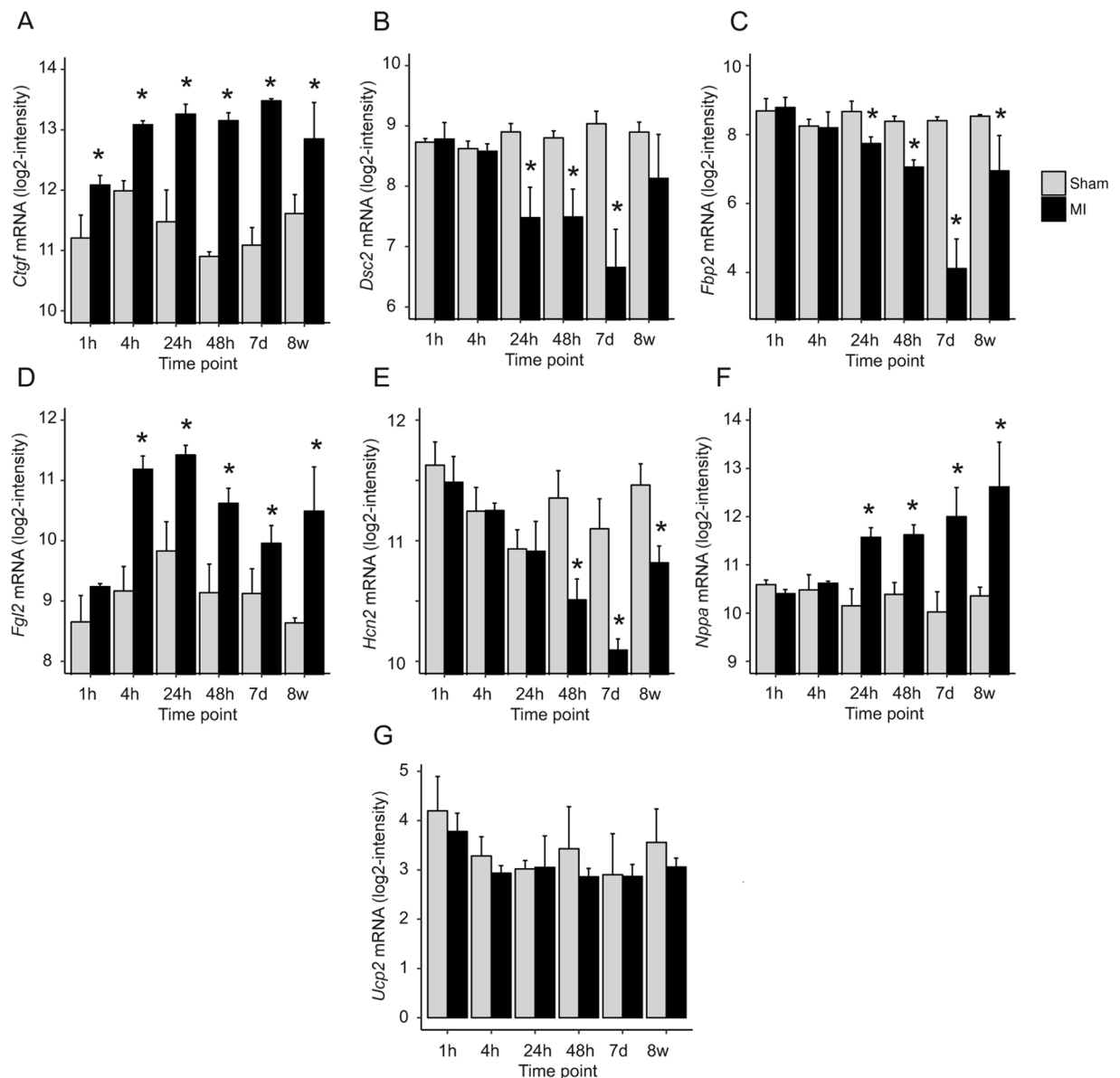


Figure 5. *In silico* gene expression analysis of candidate genes after MI. mRNA expression of *Ctgf*, *Dsc2*, *Fbp2*, *Fgl2*, *Hcn2*, *Nppa* and *Ucp2* was measured in log₂ microarray light intensity at 1 h, 4 h, 24 h, 48 h, 7 days and 8 weeks after experimentally induced MI. The GEO dataset GSE775 (Mouse model of myocardial infarction) was used. *P < 0.05 versus sham. Abbreviations: MI, myocardial infarction.

metabolism and plays a role in the control of mitochondria-derived reactive oxygen species (ROS)²⁰. Increasing evidence suggests that UCPs could play a protective role in myocardial function by reducing mitochondrial ROS generation and cardiomyocyte apoptosis²¹. Up-regulation of *Ucp2* mRNA might be an adaptive mechanism, allowing the cardiac myocytes to compensate for the higher ROS production in *AGAT*^{-/-} mice.

We showed that two genes (*Nppa*, *Ctgf*) involved in cardiac hypertrophy and fibrosis were de-regulated in *AGAT*^{-/-} animals. The protein encoded by the *Nppa* gene is atrial natriuretic peptide (ANP), which in turn predicts cardiovascular outcomes and is a biomarker of hypertrophy²². An up-regulation of *Nppa* mRNA may indicate the presence of a molecular programme of hypertrophy. However, this finding has to be critically evaluated since another study showed that not all molecular markers of cardiac hypertrophy were consistently elevated in *AGAT*^{-/-} mice, i.e., unchanged mRNA expression of brain natriuretic peptide (BNP) and beta myosin heavy chain (β -MHC) and reduced mRNA expression of alpha skeletal actin (α -SA)¹⁵. Our results additionally identified *Ctgf* mRNA to be significantly up-regulated in response to the knock-out. Previous studies showed that the encoded protein CTGF is up-regulated in cardiac cells after MI and in advanced atherosclerosis^{23–25}. In addition, CTGF may be a key regulator of fibrosis during remodelling and progression to heart failure²⁶. It does demonstrate that *AGAT* deficiency may be associated with fibrosis.

Another large proportion of candidate genes de-regulated in AGAT deficiency are associated with the cardiac conduction system. Pacemaker activity and electrical propagation may be directly affected by ion channel de-regulation (*Hcn2*, *Hcn4*, *Scn4a*, *Scn4b*) or indirectly affected (*Ehd4*) or may be affected by structural alterations (*Dsc2*). *Scn4a* and *Scn4b* mutations and expression changes have been shown to be associated with arrhythmia and tightly regulated expression of these channels is required for physiological conduction^{27–29}. Both channels were significantly down-regulated in AGAT^{-/-} mice. *Hcn2* and *Hcn4* are coding for HCN channels mediating the so-called funny current (I_f) which plays a key role in the generation and modulation of cardiac automaticity³⁰. HCN4 is highly expressed in the sinoatrial node and responsible for heart rhythm generation through spontaneous diastolic depolarization³¹. Though HCN2 is not as robustly expressed in the heart, it additionally contributes to spontaneous rhythmic activity³². The cardiac-specific knock-out of *Hcn4* in mice leads to the development of bradycardia as pacemaking activity in these animals solely relies on calcium clock mechanisms³³. In line with those data, AGAT^{-/-} mice in which *Hcn4* mRNA is down-regulated exhibited a lower maximal heart rate compared to WT littermates¹⁵. *Ehd4* mRNA was up-regulated in AGAT^{-/-} mice. Given that previous studies revealed that the EHD4 protein is enhanced in cells from the infarcted heart and related to reduced expression of cardiac sodium channels causing cardiac arrhythmias³⁴, the described up-regulation may indicate a susceptibility of AGAT^{-/-} mice to arrhythmias. Structural alterations in the heart may also cause cardiac arrhythmias. Mutations in the *Dsc2* gene, encoding a desmosome-related protein, lead to abnormalities in cardiac structure and are involved in the development of arrhythmogenic cardiomyopathy^{35,36}. *Dsc2* mRNA was significantly de-regulated in AGAT^{-/-} littermates.

We further observed de-regulated genes in AGAT^{-/-} mice that are not commonly associated with CVD. However, there is evidence that these genes may influence cardiac function. In a diabetes mouse model *Fgl2* gene silencing inhibits apoptosis and improves heart function by probably modulating immune response³⁷. *Rpp25* that was selected based on statistical significance needs further validation of an involvement in CVD.

To confirm previously described associations of our candidates with CVD, we performed *in silico* analysis in an experimental mouse model of MI. Using the available data, we were able to show a de-regulation of *Ctgf*, *Dsc2*, *Fbp2*, *Fgl2*, *Hcn2* and *Nppa* at various time points after MI. These results are compatible with the idea that a de-regulation of our candidate genes plays a role in cardiac (dys)function and CVD.

Considering that both creatine and HA are involved in cardiac (dys)function, we performed additional analyses to differentiate between creatine- and HA-dependent effects on the gene expression. We found that on gene expression level creatine rather than HA restored cardiac gene expression towards the WT. Previously, our group showed that AGAT deficiency results in disturbed energy metabolism in the muscle^{9,38}. As expected from these studies, a de-regulation of energy-related genes in the heart was reversible by creatine supplementation. Regarding cardiac function, our AGAT^{-/-} mice exhibited a cardiovascular phenotype of LVESP, impaired contractility and relaxation, as well as a lower maximal heart rate and contractile reserve¹⁵. LVESP was corrected by creatine supplementation which may be associated with a creatine-dependent regulation of *Ctgf* and *Nppa*. This finding is important as LVESP also affects the peripheral cardiovascular system.

However, all other measured parameters of cardiac function in AGAT^{-/-} mice were normalized by HA supplementation. Additionally, HA supplementation in a WT mouse model of post-MI heart failure attenuated the impaired cardiac function underlining a positive effect of HA on the cardiovascular system¹⁶. On gene expression level, our data cannot explain the underlying mechanisms of HA effect on cardiac function. We therefore assume that HA may influence the cardiac system through other mechanisms such as post-translational changes or may mainly affect other areas of the heart except the left ventricle as described below.

A limitation of our study was the exclusive use of left ventricular heart tissue. It can thus be assumed that some of the transcriptomic changes that determine the cardiac phenotype of AGAT^{-/-} mice in the other chambers have been systematically overlooked. In addition, the correlation of gene expression and protein abundance is a critical point in research, especially when using high-throughput methods. Therefore, further analysis and detailed assessment of target genes identified in our transcriptome analyses such as protein and/or metabolome analysis have to be performed. Moreover, experiments in AGAT^{-/-} CVD models (e.g., MI or heart failure) will directly link AGAT deficiency with CVD.

Taken together, our study provides first transcriptomic data on the molecular background of the AGAT metabolism and the influence of creatine and HA on molecular pathways regarding cardiac (dys)function. However, the protective mechanisms of HA in the cardiovascular system will require functions experiments.

Methods

Care and treatment of mice. AGAT^{-/-} mice were generated as previously described¹⁴. Mice used in this study were obtained from heterozygous breeding after backcrossing to a C57BL/6J genetic background for at least six generations. All analysed animals were littermates. The mice (<5 per cage) were kept in standard cages under a 12 h:12 h light:dark cycle, constant temperature and humidity and received standard food and water ad libitum. Animal chow was essentially free of creatine¹⁴. Previously, no creatine and phosphocreatine could be detected in the heart of AGAT^{-/-} mice¹⁵. HA supplementation was achieved with osmotic mini pumps for 4 weeks, as previously described¹². Creatine supplementation was achieved by addition of 1% creatine to chow (Ssniff) as previously described¹⁴. All experimental procedures were approved by the respective local animal ethics committees (Behörde für Gesundheit und Verbraucherschutz Hamburg, approval no. 110/10) and investigations applied to the animal model were conformed to the guidelines for the care and use of laboratory animals published by the NIH (Publication No. 85–23, revised 1985).

Tissue collection and preparation. Tissue collection and preparation were performed as previously described¹⁴. Briefly, mice were anesthetized with 2–3% isoflurane in 100% oxygen. After median thoracotomy the

left ventricle of the heart was extracted, and shock frozen in liquid nitrogen for storage at -80°C . Prior to use, frozen tissue was powdered with a steel mortar and pestle in liquid nitrogen.

RNA isolation from murine tissue. RNA isolation was performed using QIAzol lysis reagent. Briefly, frozen tissue powder was minced in QIAzol and further disrupted using a pellet pestle. To extract RNA, chloroform was added, mixed, and centrifuged. The aqueous phase containing the RNA was collected and isopropanol was added. For precipitation, the RNA solution was centrifuged 15 min at 4°C at high speed. After washing with 80% ethanol twice, the RNA pellet was dissolved in nuclease-free water. RNA concentration was determined by measuring absorbance at 260 nm using Nanodrop and stored at -80°C until utilization.

Gene expression analysis by microarray. Total RNA from left ventricular heart tissue was prepared in four groups of mice: WT ($n = 7$), AGAT $^{-/-}$ ($n = 7$), AGAT $^{-/-}$ HA ($n = 5$) and AGAT $^{-/-}$ Cr ($n = 4$) mice. All groups of mice were analysed at the same time. RNA integrity was assessed on a 2100 Agilent Bioanalyzer (Agilent Technologies, Germany). The Affymetrix Mouse GeneChip ST 1.0 Array was used to assess the gene expression profile. Briefly, cRNA synthesis, labelling, fragmentation, array hybridization, washing and staining, and microarray scanning (Affymetrix GeneChip 3000 scanner) was performed according to manufacturer's instruction of the Ambion WT Expression Kit and the Affymetrix GeneChip WT Terminal Labelling and Hybridization Kit with an input of 250 ng high quality RNA (RIN > 8).

Reverse transcription and quantitative polymerase chain reaction (qPCR). Reverse transcription and qPCR were performed as previously described³⁹. One μg of total RNA was reverse transcribed using the High Capacity Kit (Life Technologies). For reverse transcription, samples were incubated for 2 hours at 37°C followed by an inactivation step of 5 minutes at 85°C . Finally, cDNA was diluted in water to a final concentration of 5 ng/ μL . The relative quantification of mRNA levels was carried out on a 7900 TaqMan system (Applied Biosystems). To assess mRNA expression of target genes, real-time PCR was performed using 5 μL of the gene expression master mix (Thermo Fisher) and 0.5 μL of the gene expression assay (see Supplementary Table S4). Each gene expression assay includes forward and reverse primers as well as the FAM-labelled probe. As template 2 μL of cDNA was used in a final volume of 10 μL to detect. Each sample was analysed in duplicates and normalized to 18 S rRNA as endogenous control.

Network analysis. Clusters (modules) of highly correlated genes were identified by weighted correlation network analysis (WGCNA)⁴⁰. The so-called *eigengene* was computed for each module by calculating the first principal component based on all genes in the respective module. Associations between *eigengenes* of each module and genotype (WT and AGAT $^{-/-}$) were calculated to identify modules highly de-regulated in AGAT $^{-/-}$ compared to WT mice.

WEB-based GENE SeT Analysis Toolkit (WebGestalt). WebGestalt (www.webgestalt.org/) is a publicly available analysis toolkit for functional genomic, proteomic and large-scale genetic studies from which large number of gene lists are continuously generated⁴¹. Pathway analyses (WikiPathways) of differentially expressed gene sets were performed in order to identify an enrichment of genes in metabolic or disease-related pathways. The gene sets are adjusted for multiple testing based on the Benjamini-Hochberg method and a significance level of ≤ 0.05 was set for statistical significance.

Gene expression omnibus (GEO). To identify specific gene expression changes in MI, a systematic search in the GEO database⁴² was carried out. The keywords used for the GEO database search were: “myocardial infarction” AND “expression profiling by array” for “study type” AND “tissue” for “attribute name” AND “mus musculus” for “organism”. The GEO dataset GSE775¹⁷ was selected, which is a time series (1 hour, 4 hours, 24 hours, 48 hours, 1 week, and 8 weeks) intended to compare normal functioning left ventricles with infarcted left ventricles in mice. Expression profiling was performed based on the Affymetrix Murine Genome U74A Version 2 Array. MI has been mimicked by permanent ligation of the left coronary artery. Group comparison was performed using hearts subjected to MI (ilv) or the sham operation (lv and lv2). Raw data (CEL file) were downloaded and bioinformatics analysis were performed as described in the subsection “bioinformatics analysis”.

Bioinformatics analysis. Differential gene expression analyses of murine transcriptomes were performed using the statistical language R and R/Bioconductor (www.bioconductor.org) packages *xps* and *limma*. Microarrays were pre-processed using the package *xps*. The *rma* function was used for background correction and normalization in order to reduce variation between arrays. The detection above background (DABG) was calculated for all genes and samples, and only genes with a DABG P value < 0.01 in at least two samples per group were kept for further analysis. The moderated t-test function *eBayes* from the *limma* package was used to calculate differential gene expression between groups. The False-Discovery-Rate (FDR) based Benjamini-Hochberg method was used to account for multiple tests, and the significance level for differentially expressed genes was set to a FDR ≤ 0.05 .

Statistical analysis. The mRNA levels were quantified according to the $2^{-\Delta\Delta\text{Ct}}$ method by Livak and Schmittgen⁴³. For comparison of multiple groups, nonparametric Kruskal-Wallis-Test was used due to small sample sizes. Differences were considered statistically significant at a value of $P \leq 0.05$. All calculations were performed using Graph Pad Prism 7.

Data availability

Data, related documents such as study protocol and statistical analysis will be shared upon request from any qualified investigator for 3 years after the date of publication.

Received: 21 November 2019; Accepted: 6 February 2020;

Published online: 16 March 2020

References

1. Townsend, N. *et al.* Cardiovascular disease in Europe: epidemiological update 2016. *Eur. heart J.* **37**, 3232–3245, <https://doi.org/10.1093/eurheartj/ehw334> (2016).
2. Lloyd-Jones, D. M. Cardiovascular risk prediction: basic concepts, current status, and future directions. *Circulation* **121**, 1768–1777, <https://doi.org/10.1161/CIRCULATIONAHA.109.849166> (2010).
3. Lewis, G. D., Asnani, A. & Gerszten, R. E. Application of metabolomics to cardiovascular biomarker and pathway discovery. *J. Am. Coll. Cardiol.* **52**, 117–123, <https://doi.org/10.1016/j.jacc.2008.03.043> (2008).
4. Pilz, S. *et al.* Low homoarginine concentration is a novel risk factor for heart disease. *Heart* **97**, 1222–1227, <https://doi.org/10.1136/hrt.2010.220731> (2011).
5. Atzler, D., Schwedhelm, E. & Choe, C. U. L-homoarginine and cardiovascular disease. *Curr. Opin. Clin. Nutr. Metab. Care* **18**, 83–88, <https://doi.org/10.1097/MCO.000000000000123> (2015).
6. Atzler, D. *et al.* Low Homoarginine Levels in the Prognosis of Patients With Acute Chest Pain. *J. Am. Heart Assoc.* **5**, e002565, <https://doi.org/10.1161/JAHA.115.002565> (2016).
7. Hrabak, A., Bajor, T. & Temesi, A. Comparison of substrate and inhibitor specificity of arginase and nitric oxide (NO) synthase for arginine analogues and related compounds in murine and rat macrophages. *Biochem. Biophys. Res. Commun.* **198**, 206–212 (1994).
8. Karetnikova, E. S. *et al.* Is Homoarginine a Protective Cardiovascular Risk Factor? *Arterioscler. Thromb. Vasc. Biol.* **39**, 869–875, <https://doi.org/10.1161/ATVBAHA.118.312218> (2019).
9. Nabuurs, C. I. *et al.* Disturbed energy metabolism and muscular dystrophy caused by pure creatine deficiency are reversible by creatine intake. *J. Physiol.* **591**, 571–592, <https://doi.org/10.1113/jphysiol.2012.241760> (2013).
10. Neubauer, S. The failing heart—an engine out of fuel. *N. Engl. J. Med.* **356**, 1140–1151, <https://doi.org/10.1056/NEJMra063052> (2007).
11. Lygate, C. A. *et al.* The creatine kinase energy transport system in the failing mouse heart. *J. Mol. Cell Cardiol.* **42**, 1129–1136, <https://doi.org/10.1016/j.yjmcc.2007.03.899> (2007).
12. Choe, C. U. *et al.* Homoarginine levels are regulated by L-arginine:glycine amidinotransferase and affect stroke outcome: results from human and murine studies. *Circulation* **128**, 1451–1461, <https://doi.org/10.1161/CIRCULATIONAHA.112.000580> (2013).
13. Kleber, M. E. *et al.* Genome-wide association study identifies 3 genomic loci significantly associated with serum levels of homoarginine: the AtheroRemo Consortium. *Circ. Cardiovasc. Genet.* **6**, 505–513, <https://doi.org/10.1161/CIRCGENETICS.113.000108> (2013).
14. Choe, C. U. *et al.* L-arginine:glycine amidinotransferase deficiency protects from metabolic syndrome. *Hum. Mol. Genet.* **22**, 110–123, <https://doi.org/10.1093/hmg/dds407> (2013).
15. Faller, K. M. E. *et al.* Impaired cardiac contractile function in arginine:glycine amidinotransferase knockout mice devoid of creatine is rescued by homoarginine but not creatine. *Cardiovasc. Res.* **114**, 417–430, <https://doi.org/10.1093/cvr/cvx242> (2018).
16. Atzler, D. *et al.* Dietary Supplementation with Homoarginine Preserves Cardiac Function in a Murine Model of Post-Myocardial Infarction Heart Failure. *Circulation* **135**, 400–402, <https://doi.org/10.1161/CIRCULATIONAHA.116.025673> (2017).
17. Tarnavski, O. *et al.* Mouse cardiac surgery: comprehensive techniques for the generation of mouse models of human diseases and their application for genomic studies. *Physiol. Genomics* **16**, 349–360, <https://doi.org/10.1152/physiolgenomics.00041.2003> (2004).
18. Atzler, D. *et al.* Homoarginine and cardiovascular outcome in the population-based Dallas Heart Study. *Arterioscler. Thromb. Vasc. Biol.* **34**, 2501–2507, <https://doi.org/10.1161/ATVBAHA.114.304398> (2014).
19. Fearnley, C. J., Roderick, H. L. & Bootman, M. D. Calcium signaling in cardiac myocytes. *Cold Spring Harb. Perspect. Biol.* **3**, a004242, <https://doi.org/10.1101/cshperspect.a004242> (2011).
20. Saleh, M. C., Wheeler, M. B. & Chan, C. B. Uncoupling protein-2: evidence for its function as a metabolic regulator. *Diabetologia* **45**, 174–187, <https://doi.org/10.1007/s00125-001-0737-x> (2002).
21. Akhmedov, A. T., Rybin, V. & Marin-Garcia, J. Mitochondrial oxidative metabolism and uncoupling proteins in the failing heart. *Heart Fail. Rev.* **20**, 227–249, <https://doi.org/10.1007/s10741-014-9457-4> (2015).
22. Wang, T. J. *et al.* Plasma natriuretic peptide levels and the risk of cardiovascular events and death. *N. Engl. J. Med.* **350**, 655–663, <https://doi.org/10.1056/NEJMoa031994> (2004).
23. Ohnishi, H. *et al.* Increased expression of connective tissue growth factor in the infarct zone of experimentally induced myocardial infarction in rats. *J. Mol. Cell Cardiol.* **30**, 2411–2422, <https://doi.org/10.1006/jmcc.1998.0799> (1998).
24. Ahmed, M. S. *et al.* Connective tissue growth factor—a novel mediator of angiotensin II-stimulated cardiac fibroblast activation in heart failure in rats. *J. Mol. Cell Cardiol.* **36**, 393–404, <https://doi.org/10.1016/j.yjmcc.2003.12.004> (2004).
25. Oemar, B. S. *et al.* Human connective tissue growth factor is expressed in advanced atherosclerotic lesions. *Circulation* **95**, 831–839 (1997).
26. Koshman, Y. E. *et al.* Regulation of connective tissue growth factor gene expression and fibrosis in human heart failure. *J. Card. Fail.* **19**, 283–294, <https://doi.org/10.1016/j.cardfail.2013.01.013> (2013).
27. Coronel, R. *et al.* Cardiac expression of skeletal muscle sodium channels increases longitudinal conduction velocity in the canine 1-week myocardial infarction. *Heart Rhythm* **7**, 1104–1110, <https://doi.org/10.1016/j.hrthm.2010.04.009> (2010).
28. Lau, D. H. *et al.* Epicardial border zone overexpression of skeletal muscle sodium channel SkM1 normalizes activation, preserves conduction, and suppresses ventricular arrhythmia: an in silico, in vivo, in vitro study. *Circulation* **119**, 19–27, <https://doi.org/10.1161/CIRCULATIONAHA.108.809301> (2009).
29. Li, R. G. *et al.* Mutations of the SCN4B-encoded sodium channel beta4 subunit in familial atrial fibrillation. *Int. J. Mol. Med.* **32**, 144–150, <https://doi.org/10.3892/ijmm.2013.1355> (2013).
30. Robinson, R. B. & Siegelbaum, S. A. Hyperpolarization-activated cation currents: from molecules to physiological function. *Annu. Rev. Physiol.* **65**, 453–480, <https://doi.org/10.1146/annurev.physiol.65.092101.142734> (2003).
31. DiFrancesco, D. The role of the funny current in pacemaker activity. *Circ. Res.* **106**, 434–446, <https://doi.org/10.1161/CIRCRESAHA.109.208041> (2010).
32. Vaccari, T. *et al.* The human gene coding for HCN2, a pacemaker channel of the heart. *Biochim. Biophys. Acta* **1446**, 419–425 (1999).
33. Baruscotti, M. *et al.* Deep bradycardia and heart block caused by inducible cardiac-specific knockout of the pacemaker channel gene Hcn4. *Proc. Natl Acad. Sci. USA* **108**, 1705–1710, <https://doi.org/10.1073/pnas.1010122108> (2011).
34. Dun, W., Danilo, P. Jr., Mohler, P. J. & Boyden, P. A. Microtubular remodeling and decreased expression of Nav1.5 with enhanced EHD4 in cells from the infarcted heart. *Life Sci.* **201**, 72–80, <https://doi.org/10.1016/j.lfs.2018.03.024> (2018).
35. Sun, C., Wang, L., Yang, X. X., Jiang, Y. H. & Guo, X. L. The aberrant expression or disruption of desmocolin2 in human diseases. *Int. J. Biol. Macromol.* **131**, 378–386, <https://doi.org/10.1016/j.ijbiomac.2019.03.041> (2019).

36. Brodehl, A. *et al.* Transgenic mice overexpressing desmocollin-2 (DSC2) develop cardiomyopathy associated with myocardial inflammation and fibrotic remodeling. *PLoS One* **12**, e0174019, <https://doi.org/10.1371/journal.pone.0174019> (2017).
37. Zhenzhong, Z., Yafa, Y. & Jin, L. Fibrinogen-like protein 2 gene silencing inhibits cardiomyocytes apoptosis, improves heart function of streptozotocin-induced diabetes rats and the molecular mechanism involved. *Biosci Rep* **35**, <https://doi.org/10.1042/BSR20150078> (2015).
38. Stockebrand, M. *et al.* Transcriptomic and metabolic analyses reveal salvage pathways in creatine-deficient AGAT(−/−) mice. *Amino Acids* **48**, 2025–2039, <https://doi.org/10.1007/s00726-016-2202-7> (2016).
39. Lindner, D. *et al.* Cardiac fibroblasts aggravate viral myocarditis: cell specific coxsackievirus B3 replication. *Mediators Inflamm.* **2014**, 519528, <https://doi.org/10.1155/2014/519528> (2014).
40. Langfelder, P. & Horvath, S. WGCNA: an R package for weighted correlation network analysis. *BMC Bioinforma.* **9**, 559, <https://doi.org/10.1186/1471-2105-9-559> (2008).
41. Zhang, B., Kirov, S. & Snoddy, J. WebGestalt: an integrated system for exploring gene sets in various biological contexts. *Nucleic Acids Res.* **33**, W741–748, <https://doi.org/10.1093/nar/gki475> (2005).
42. Edgar, R., Domrachev, M. & Lash, A. E. Gene Expression Omnibus: NCBI gene expression and hybridization array data repository. *Nucleic Acids Res.* **30**, 207–210 (2002).
43. Livak, K. J. & Schmittgen, T. D. Analysis of relative gene expression data using real-time quantitative PCR and the 2^{−(Delta Delta C(T))} Method. *Methods* **25**, 402–408, <https://doi.org/10.1006/meth.2001.1262> (2001).
44. Willner, N., Goldberg, Y., Schiff, E. & Vadasz, Z. Semaphorin 4D levels in heart failure patients: a potential novel biomarker of acute heart failure? *ESC Heart Fail.* **5**, 603–609, <https://doi.org/10.1002/ehf2.12275> (2018).
45. Song, Z. *et al.* Essential role for UVRAG in autophagy and maintenance of cardiac function. *Cardiovasc. Res.* **101**, 48–56, <https://doi.org/10.1093/cvr/cvt223> (2014).

Acknowledgements

Märít Jensen was supported by a scholarship from the Cardiovascular Research Centre (CVRC) of the University Medical Centre Hamburg-Eppendorf. Tanja Zeller was supported by research grants from the German Centre of Cardiovascular Research (FKZ 81Z1710101, FKZ 81Z07410102).

Author contributions

M.J. performed the experiments, interpreted the results, created the figures and wrote the manuscript text; C.M. performed statistical analysis; C.C. supervised the animal experiments, interpreted the results and created the figures; E.S. supervised the animal experiments and interpreted the results; T.Z. supervised the project, interpreted the results and wrote the manuscript text. All authors reviewed the manuscript.

Competing interests

Chi-un Choe received lecture fees from Pfizer. The other authors declare no competing interests.

Additional information

Supplementary information is available for this paper at <https://doi.org/10.1038/s41598-020-61638-3>.

Correspondence and requests for materials should be addressed to T.Z.

Reprints and permissions information is available at www.nature.com/reprints.

Publisher's note Springer Nature remains neutral with regard to jurisdictional claims in published maps and institutional affiliations.



Open Access This article is licensed under a Creative Commons Attribution 4.0 International License, which permits use, sharing, adaptation, distribution and reproduction in any medium or format, as long as you give appropriate credit to the original author(s) and the source, provide a link to the Creative Commons license, and indicate if changes were made. The images or other third party material in this article are included in the article's Creative Commons license, unless indicated otherwise in a credit line to the material. If material is not included in the article's Creative Commons license and your intended use is not permitted by statutory regulation or exceeds the permitted use, you will need to obtain permission directly from the copyright holder. To view a copy of this license, visit <http://creativecommons.org/licenses/by/4.0/>.

© The Author(s) 2020